

Research Article

Cite this article: Reunov A *et al.* (2020) Germ plasm-related structures in marine medaka gametogenesis; novel sites of Vasa localization and the unique mechanism of germ plasm granule arising. *Zygote* **28**: 9–23. doi: [10.1017/S0967199419000546](https://doi.org/10.1017/S0967199419000546)

Received: 16 April 2019

Revised: 3 August 2019

Accepted: 20 August 2019

First published online: 8 October 2019

Keywords:

Germ plasm formation; Germ plasm-related structures; Marine medaka; Meiotic differentiation; Oogenesis; Spermatogenesis; Vasa

Address for correspondence:

Arkadiy Reunov. St. Francis Xavier University, Department of Biology, Antigonish, NS B2G 2W5, Canada. E-mail: areunov@stfx.ca

Germ plasm-related structures in marine medaka gametogenesis; novel sites of Vasa localization and the unique mechanism of germ plasm granule arising

Arkadiy A. Reunov^{1,2} , Doris W. T. Au³, Yana N. Alexandrova¹, Michael W. L. Chiang³ , Miles T. Wan³, Konstantin V. Yakovlev¹, Yulia A. Reunova¹, Alina V. Komkova¹, Napo K. M. Cheung³, Drew R. Peterson³ and Andrey V. Adrianov^{1,4}

¹National Scientific Centre of Marine Biology, Far Eastern Branch, Russian Academy of Sciences, Vladivostok, 690041; Russia; ²St. Francis Xavier University, Department of Biology, Antigonish, NS B2G 2W5, Canada; ³State Key Laboratory of Marine Pollution, Department of Chemistry, City University of Hong Kong, 83 Tat Cher Avenue, Kowloon, Hong Kong and ⁴Far Eastern Federal University, School of Natural Sciences, 10 Ajax Bay, Russky Island, Vladivostok 690950, Russia

Summary

Germ plasm, a cytoplasmic factor of germline cell differentiation, is suggested to be a perspective tool for *in vitro* meiotic differentiation. To discriminate between the: (1) germ plasm-related structures (GPRS) involved in meiosis triggering; and (2) GPRS involved in the germ plasm storage phase, we investigated gametogenesis in the marine medaka *Oryzias melastigma*. The GPRS of the mitosis-to-meiosis period are similar in males and females. In both sexes, five events typically occur: (1) turning of the primary Vasa-positive germ plasm granules into the Vasa-positive intermitochondrial cement (IMC); (2) aggregation of some mitochondria by IMC followed by arising of mitochondrial clusters; (3) intramitochondrial localization of IMC-originated Vasa; followed by (4) mitochondrial cluster degradation; and (5) intranuclear localization of Vasa followed by this protein entering the nuclei (gonial cells) and synaptonemal complexes (zygotene–pachytene meiotic cells). In post-zygotene/pachytene gametogenesis, the GPRS are sex specific; the Vasa-positive chromatoid bodies are found during spermatogenesis, but oogenesis is characterized by secondary arising of Vasa-positive germ plasm granules followed by secondary formation and degradation of mitochondrial clusters. A complex type of germ plasm generation, ‘the follicle cell assigned germ plasm formation’, was found in late oogenesis. The mechanisms discovered are recommended to be taken into account for possible reconstruction of those under *in vitro* conditions.

Introduction

Generation of artificial gametes is demanded in reproductive technologies. Some progress has been achieved with stem cell transformation into sperm and oocytes. However, no reliable approaches for meiotic differentiation exist yet. The main problem is insufficient knowledge of the mechanisms that provide viable meiosis triggering and progression. Studies of the gamete differentiation mechanisms occurring in the gonads of model animals appear to be basic to support *in vitro* technologies (Kashir *et al.*, 2012; Medrano *et al.*, 2013; Hendriks *et al.*, 2015; Moreno *et al.*, 2015; Nikolic *et al.*, 2016).

Germ plasm is still an unclaimed but necessary tool for meiotic differentiation

It is worth noting that in the course of the ongoing experiments on meiotic determination of stem cells, some external factors were taken into account such as stem cell co-culture with the feeder cells, influence of embryonic tissue on transplanted grafts from adult gonads, effect of primordial germ-cell number, variation of growth factor, modification of culture medium, and improvements of culture conditions (Sakai, 2002; Kawasaki *et al.*, 2010, 2012, 2016; Riesco *et al.*, 2014; Tzung *et al.*, 2014). However, there is an intrinsic germ-cell fate element known as ‘germ plasm’. This element has not yet been the focus of reproductive technologies.

Germ plasm is a cytoplasmic substance acting as a factor of germline cell differentiation (Saffman and Lasko, 1999). To date, it has been known that germ plasm is formed and stored during oogenesis with the involvement of the mitochondrial cloud, also known as the Balbiani body (Kalt, 1973; Kloc *et al.*, 2002; Cox and Spradling, 2003; Chang *et al.*, 2004; Wilk *et al.*, 2004). The germ plasm is referred to as polar granules in *Drosophila* (Mahowald, 1962), germinal granules in *Xenopus* (Kloc *et al.*, 2002; Chang *et al.*, 2004),

and P granules in *Caenorhabditis elegans* (Strome and Wood, 1983; Wolf et al. 1983). Following the formation in oocytes/eggs/early embryos, and eventual incorporation into primordial germ cells (PGC), the germ plasm granules (GG) are segregated throughout embryogenesis and play some role in meiotic differentiation of mitotically multiplying germline stem cells of the new generation in the gonads of both sexes (Williamson and Lehmann, 1996; Matova and Cooley, 2001; Carré et al., 2002; Milani et al., 2017). Therefore, there are two phases of germ plasm state: (1) the 'storage phase' including GG formation and transportation during oogenesis/embryogenesis; and (2) the 'phase of mitosis-to-meiosis shift' occurring during early gametogenesis in the gonad niche. Further elucidation of the cellular and subcellular mechanisms that underlie both germ plasm phases is of high importance in a reproductive technology.

Vasa is a main germ plasm component with an unclear role

The *vasa* gene encoding an ATF-dependent RNA helicase of the DEAD-box protein family was discovered in *Drosophila* (Lasko and Ashburner, 1988; Hay et al. 1990). Its analogues have been also found in a number of invertebrate and vertebrate animal species (Raz, 2000; Toyooka et al., 2000; Mochizuki et al., 2001; Sunagara et al., 2006) and human (Castrillon et al., 2000). All of the *vasa* homologue genes undergo expression in germline cells and usually reside in the GG (Carré et al., 2002). *Vasa* protein is a key germ plasm component (Findley et al., 2003), however its function remains obscure in terms of establishment and maintenance of germline cells (Gustafson and Wessel, 2010). A more detailed knowledge of the *Vasa* role in both germ plasm phases is required.

Germ plasm and vasa in fishes

In fish, the importance of artificial germline cell setting up is increasing in connection with restoration of extinct species and conservation of endemic and commercially valuable species (Higaki et al., 2017). Fish germ plasm has been the subject of study in both the storage and mitosis-to-meiosis phases.

For the storage phase, it is unclear how GG are formed. Although the *bucky ball* (*buc*) gene, which is universally involved in Balbiani body formation, was detected in zebrafish oogenesis, and a Balbiani body-like cloud was visualized by immunolight microscopy (Bontems et al., 2009), an ultrastructural mechanism of germ plasm formation has not been described yet in any fish species. It is known that in the freshwater medaka *Oryzias latipes*, zebrafish *Danio rerio* and some other teleost fishes the GG, termed 'germinal dense bodies' or 'nuage', are initially segregated during late oogenesis or very early embryogenesis (gastrulation or epiboly), transferred through embryogenesis by PGC, and are finally inherited by gonial germ cells that represent a gonadal stage of PGC differentiation (Hamaguchi, 1982, 1985; Timmermans and Taverne, 1989; Braat et al., 1999). Knaut et al. (2000) reported that in zebrafish the numerous small germ plasm particles are registered in the 1-cell stage embryos in close proximity to the cortical actin, and that these particles contain *vasa* RNA but not *Vasa* protein. During embryogenesis, maternally provided (zygotic) *Vasa* has been identified as a component of the PGC (Hartung et al., 2014). *Vasa* localization in adult germline cells was reported for zebrafish *Danio rerio* (Braat et al., 1999; Knaut et al., 2000), and tilapia (Kobayashi et al., 2000). Using electron microscopy, it was shown that *Vasa* localizes in GG during

gametogenesis of the gibel carp *Carassius auratus gibelio* (Xu et al., 2005) and freshwater medaka *O. latipes* (Yuan et al., 2014).

For the mitosis-to-meiosis phase, it has been reported for *O. latipes* that GG are present in germline stem cells during gonad formation (Hamaguchi, 1982, 1985). In *O. latipes*, *Poecilia reticulata* and teleost fish of the genus *Xiphophorus*, the embryonic PGC and adult germ cells (oogonia and spermatogonia) were reported as having polymorphic GG such as 'electron-dense granular material', 'nuage', and 'intermitochondrial cement' (IMC) (Satoh, 1974; Billard, 1984; Flores and Burns, 1993; Braat et al., 1999). However, it is unclear if GG are involved in mitosis-to-meiosis shift. For meiosis promotion, it has been suggested that differentiation of germ cells is passive and determined by accessory cells that surround the oogonia in the mature ovary and the early spermatogonia in the mature testis (Flores and Burns, 1993, and references therein). However, as GG represent an actually significant morphologic component of premeiotic cells, it seems reasonable to verify if GG may be involved in meiosis onset.

In terms of the *Vasa* role in mitosis-to-meiosis shift, it was noted that maternal *Vasa* mutants failed to progress beyond the pachytene stage of meiosis and lose germline cells (Hartung et al., 2014). However, it still has to be elucidated if *Vasa* is involved directly in the mitosis-to-meiosis shift. It seems relevant to find out if *Vasa* promotes meiosis as unrelated to GG or as a component of GG.

Interestingly, early germ cells in female and male fish gonads are normally not sexually determined. Indeed, in *O. latipes*, *P. reticulata*, and teleost fishes of the genus *Xiphophorus* the embryonic PGC and adult germ cells (oogonia and spermatogonia) were reported as similar in both sexes in respect to general ultrastructure (Satoh, 1974; Billard, 1984; Azevedo, 1984; Flores and Burns, 1993; Braat et al., 1999). Noteworthy, although the germline cells anticipating mitosis-to-meiosis shift are morphologically similar in both fish sexes, it remains unclear whether premeiotic GG activity may differ between the two sexes. This question seems important if *in vitro* sex-specific meiotic differentiation is targeted.

The aim of this study was to extend our knowledge concerning GG and the *Vasa* role during meiotic differentiation in spermatogenesis and oogenesis of the marine medaka *Oryzias melastigma*. We investigated *Vasa* and germ plasm-related structures (GPRS) in their dynamic localization with a focus on: (1) sex-specific difference/similarity of GPRS activity during mitosis-to-meiosis shift; (2) sex-specific difference/similarity of GPRS activity after mitosis-to-meiosis shift; and (3) mechanisms of germ plasm formation in oogenesis.

Materials and methods

Animals

The marine medaka *O. melastigma* individuals were kindly provided by the State Key Laboratory in Marine Pollution, the City University of Hong Kong. All animals were kept in optimal rearing conditions (28 ± 2°C, 30 ± 2‰, DO > 5 mg/l, pH 8.0 ± 0.2, 12-h light/12-h dark cycle). Animal maintenance and the experiments described below were reviewed and approved by the City University of Hong Kong Research Committee for its compliance with the Animals (Control of Experiments) Ordinance, Cap. 340, of the Hong Kong Special Administrative Region.

Anti-Vasa antibodies production

Anti-Vasa polyclonal antibodies were raised in rabbit against conserved the teleost Vasa sequence peptide DDILVDVSGTNPPKAIMTFEEAKLC at the Almbion company (Voronezh, Russia).

Western blot analysis

Tissues (testes and ovary) were briefly homogenized on ice in RIPA buffer supplemented with protease inhibitor. Samples were incubated on ice for 10 min to maximize protein solubilization and then centrifuged at 19,000 g at 4°C. The supernatant was saved for protein determination by Bradford assay. Protein samples were mixed with loading buffer and then denatured at 100°C for 10 min. Samples were resolved using 8% SDS-PAGE and transferred to a nitrocellulose membrane. The membrane was blocked with 5% skimmed milk in phosphate-buffered saline with 0.1% Tween 20 (PBST) for 1 h at room temperature and then incubated with primary antibodies diluted with 5% skimmed milk in 0.1% PBST overnight at 4°C. Rabbit anti-Vasa antibodies were used at a concentration of 0.1 µg/ml. The membrane was washed with PBST and incubated with horseradish peroxidase (HRP)-conjugated goat anti-rabbit antibodies (1:5000 dilution, PI-1000, Vector Laboratories, USA) for 1 h at room temperature, rinsed with PBST and PBS and then developed using the Amersham Western ECL Substrate (GE Healthcare Life Sciences, USA).

Histology

Ovaries were fixed in 2.5% glutaraldehyde in a 0.1 M cacodylate buffer and post-fixed in OsO₄ (2%) in a 0.1 M cacodylate buffer. After washing in 0.1 M cacodylate buffer, the tissues were dehydrated through an ethanol series. The material was then penetrated using an increasing series of LR White Resin diluted in alcohol. Finally, the tissues were embedded in LR White Resin. Semi-thin sections (0.5 µm) were cut on an Ultracut Leica UC6 ultramicrotome (Leica Microsystems, Germany) using a glass knife and placed onto slides. Sections were stained with methylene blue and examined under a light microscope.

Processing of whole medaka fish and immunolight microscopy

Whole medaka fish were anesthetized in ice water. GPHS fixative (0.05% glutaraldehyde–2% paraformaldehyde–80% HistoChoice containing 1% sucrose and 1% CaCl₂) was flushed over the gills and injected into the abdominal cavity through the mouth. After removing the skull roof, otoliths and fins were cut out with a scalpel, and a small hole was punched into the swim bladder to release the air inside. The body was slit open along the mid-ventral line (from the anal vent to the operculum) to facilitate rapid penetration of the fixative. The medaka were immersed in fixative for 24 h at 4°C and then dehydrated in a graded series of methanol (70%, 80%, 95% 2×, and 100% 3×) for 20 min per step, followed by clearing in chloroform three times (30 min each). The fish were then infiltrated and embedded in paraffin. Paraffin sections (5-µm thick) of fish were cut using a rotary microtome (Leica RM2125, Germany) and mounted onto Superfrost® Plus slides (Menzel-Gläser, Germany).

Tissue sections were deparaffined by immersing the slides in xylenes (5 min 3×). After rehydration in 100% ethanol, the sections were incubated in 100% methanol containing 0.3%

H₂O₂ for 15 min to quench endogenous peroxidases. For immune localization of Vasa protein, sections were first heated in an antigen retrieval medium (0.01 M citrate buffer, pH 6.0) in a microwave oven for 15 min, followed by protein blocking in 1% BSA in PBS for 30 min at room temperature. The blocking solution was then tipped off, and the sections were incubated with primary antibody (rabbit anti-Vasa, 1:200 dilution) at 37°C for 30 min. For the negative control, a 1% BSA solution in PBS was used instead of primary antibody. Treatment with the primary antibodies was followed by incubation with HRP-conjugated secondary goat anti-rabbit antibodies (1:1000 dilution, 7074P2, Cell Signalling Technologies, USA) at 37°C for 30 min. The sections were rinsed in PBS and signals were detected with the chromogenic substrate, 3,3'-diaminobenzidine chromogen (DAB) (Dako Cytomation, Denmark). The sections were counterstained with Mayer's haematoxylin (Dako Cytomation, Denmark) and mounted with Permount (Fisher Scientific). Then the sections were examined and photographed under a light microscope (Nikon Eclipse 90i, Japan) equipped with a SPOT Xplorer 4MP Slider digital imaging system (USA).

Immunoelectron microscopy

Ovaries and testes were fixed in 4% paraformaldehyde and 0.5% glutaraldehyde in a 0.1 M sodium cacodylate buffer (pH 7.4). After dehydrating the samples through increasing concentrations of ethanol, the pellets were embedded into LR White Resin. The blocks were cut on an Ultracut Leica UC6 ultramicrotome (Leica Microsystems, Germany) using a diamond knife. Thin sections were mounted on formvar-coated nickel grids. The grids were floated on drops of 1% BSA/0.01% Tween 20 in PBS for 1 h and then incubated for 1 h with primary anti-Vasa antibodies at a 1:200 concentration. Next, the samples were washed in PBST and incubated for 2 h with a mixture of secondary antibody in PBST. The secondary antibodies were 12-nm colloidal gold-conjugated goat anti-rabbit IgG antibodies (111-205-144, Jackson) that were applied in a 1:50 dilution for 2 h at room temperature. For control sample preparation, primary antibodies were omitted and only secondary antibodies were used. The grids were washed three times in PBST, rinsed in distilled water, stained with uranyl acetate and lead citrate, and observed and photographed using a Zeiss Libra 120 transmission electron microscope (Carl Zeiss Group, Germany) and Philips 410 transmission electron microscope (Philips 123 Electronics, Eindhoven, The Netherlands).

Transmission electron microscopy

Ovaries and testes were fixed in 2.5% glutaraldehyde in a 0.1 M cacodylate buffer and post-fixed in OsO₄ (2%) in a 0.1 M cacodylate buffer. After washing in the 0.1 M cacodylate buffer, the samples were dehydrated through an ethanol series. The material was then penetrated with an increasing series of LR White Resin diluted in alcohol. Finally, the tissues were embedded in LR White Resin. Ultrathin sections (80 nm) were cut on an Ultracut Leica UC6 ultramicrotome (Leica Microsystems, Germany) using a diamond knife and placed onto copper grids coated with formvar film. The sections were stained with uranyl acetate and lead citrate solutions and examined under a Zeiss Libra 120 transmission electron microscope (Carl Zeiss Group, Germany) and Philips 410 transmission electron microscope (Philips 123 Electronics, Eindhoven, The Netherlands).

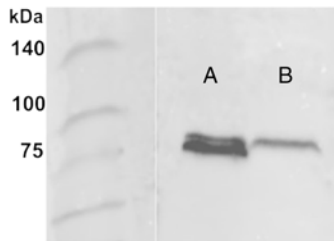


Figure 1. Western blots using anti-Vasa antibodies in the material extracted from the testes (A) and ovary (B) of the marine medaka *Oryzias melastigma*. Both the ovary and the testis have a signal of approximately 75 kDa. The testis signal consists of two bands.

GPRS quantification during meiosis induction

Three pieces of testis and three pieces of ovary were taken from each of three males and three females and embedded in resin blocks. From each of these 18 blocks (nine for females and nine for males), three sections were taken from different levels. Therefore, 54 sections were examined (27 for females and 27 for males). In each section, the presence of such GPRS as: (1) compact germinal granules; (2) loosened germinal granules; (3) mitochondrial clusters; (4) partly degraded mitochondrial clusters; and (5) degraded mitochondrial clusters were determined in 10 premeiotic cells and 10 zygotene–pachytene cells. Therefore, 540 cells for the premeiotic stage and 540 cells for the zygotene–pachytene stage, in total 1080 cells were studied. GPRS were identified by electron microscopy and counted. All values are expressed as mean values with standard error of the mean (SEM). Percentages were calculated using Student's *t*-test, and a *P*-value < 0.05 was considered statistically significant.

Results

GPRS in spermatogonia and zygotene–pachytene spermatocytes

Rabbit polyclonal antibodies against Vasa were investigated using western blot for marine medaka testes. Blots ran at the level equivalent to 75 kDa. The assay showed that the signal for the testes was represented by two blots (Fig. 1A). The Vasa signal was not found in the control staining (not shown) but was rather extensive in experimental studies using both immunolight microscopy and electron microscopy (Figs 2A–S, 4A–J, 5A–L, 6A–L, 7A–L, 8A–K, and 9A–G).

By transmission electron microscopy (TEM), we verified spermatogonia cells using such traits such as the nuclei filled with granular chromatin uniformly distributed over the nucleus and having nucleoli (Fig. 2A). Some cysts contained early spermatogenic cells that lacked the nucleoli in their nuclei and showed chromatin arranged into condensed strands. We examined the cells with chromatin strands and synaptonemal complexes to make sure that these cells were primary spermatocytes that belonged to the zygotene–pachytene stage of meiosis (Fig. 2B). Both spermatogonia and zygotene–pachytene spermatocytes were distinguished by having GG. There were compact GG that were positive for Vasa, as shown by iEM (Fig. 2A,C,D). Some Vasa-positive GG had an irregular shape and were characterized by having a loosened content (Fig. 2E). A quantitative analysis revealed that the proportions of GG patterns varied. In spermatogonia, the compact GG constituted 21.0%, and 11.0% belonged to

the loosened GG. Zygotene–pachytene spermatocytes lacked compact GG, but loosened GG constituted 6.0% (Fig. 3A).

As shown by immunohistology, the spermatogonia had a very dense Vasa signal located asymmetrically relative to its localization in the cell (Fig. 4A). The localization of GG at one of the cell poles was also shown by electron microscopy (Fig. 2A). Zygotene–pachytene spermatocytes were positive for Vasa, but, contrary to spermatogonia, the signal was more faint and distributed across the entire cytoplasm (Fig. 4B).

In both spermatogonia and zygotene–pachytene spermatocytes, the substance of the loosened GG tended to contact the nucleus. The Vasa-positive strands of these GG were found in direct connection with the nuclear membrane (Fig. 2E). Some Vasa was found in cytoplasm and in close vicinity to the nuclear membrane, inside the nuclear membrane (nuclear pores), and near the nuclear membrane inside of the nucleus (Fig. 2F). Vasa was also located in the vicinity of and inside the nucleolus (Fig. 2G and its magnification in Fig. 2H). In zygotene–pachytene spermatocytes, the Vasa was also found inside the nucleus and synaptonemal complexes (Fig. 2I). Magnification of the square outlined in Fig. 2(I) showed that Vasa is located in the light periphery of the synaptonemal complex (Fig. 2J). Also, Vasa was found directly inside the synaptonemal complex stripe (Fig. 2K).

Some spermatogonia and zygotene–pachytene spermatocytes were found with mitochondrial clusters formed by mitochondria and attached to the loosened GG, which play the role of IMC. The IMC tends to contact some neighbouring mitochondria (Fig. 2L) and at the next stage appeared as the central core collared by several mitochondria that form tight connection with the core (Fig. 2M,N). In mature mitochondrial clusters the mitochondria were profoundly introduced into the IMC and closely attached to each other (Fig. 2O). The magnification of the square outlined in Fig. 2(O) shows that Vasa was located in the IMC and inside mitochondria contacting the IMC (Fig. 2P). Vasa clusters were often found near mitochondrial membranes, between membranes, and in the vicinity of the inner membrane inside mitochondrial remnants (Fig. 2Q).

Some clustered mitochondria were typically found at various stages of degradation. A part of the mitochondrion content was autolyzed (Fig. 2R). In some clusters, the mitochondria appear as membraneous remnants having Vasa-positive substance between and inside the mitochondria (Fig. 2S).

To quantify mitochondrial clusters, we distinguished the following cluster types: 'mitochondrial cluster' (MC) (for clusters consisting of mitochondria having intact structure); 'partly degraded mitochondrial clusters' (PDMC) (for clusters having both normal and autolyzed mitochondria); and 'degraded mitochondrial clusters' (DMC) (for clusters consisting of mitochondrial remnants). Quantitative analysis revealed that the proportions of MC types varied. In spermatogonia, the mitochondrial clusters consisted of 14.0% MC, 8.0% PDMC, and 2.0% DMC (Fig. 3A). Zygotene–pachytene spermatocytes contained fewer MC (4.0%). However, there were more PDMC and DMC, comprising 16.0% and 18.0%, respectively (Fig. 3A).

GPRS in spermatids and sperms

More advanced stages of spermatogenesis such as spermatids and spermatozoa were identified based on cell size. Spermatids were smaller compared with early spermatogenic cells (Fig. 4C). Spermatozoa had a cell size smaller than the size of spermatids

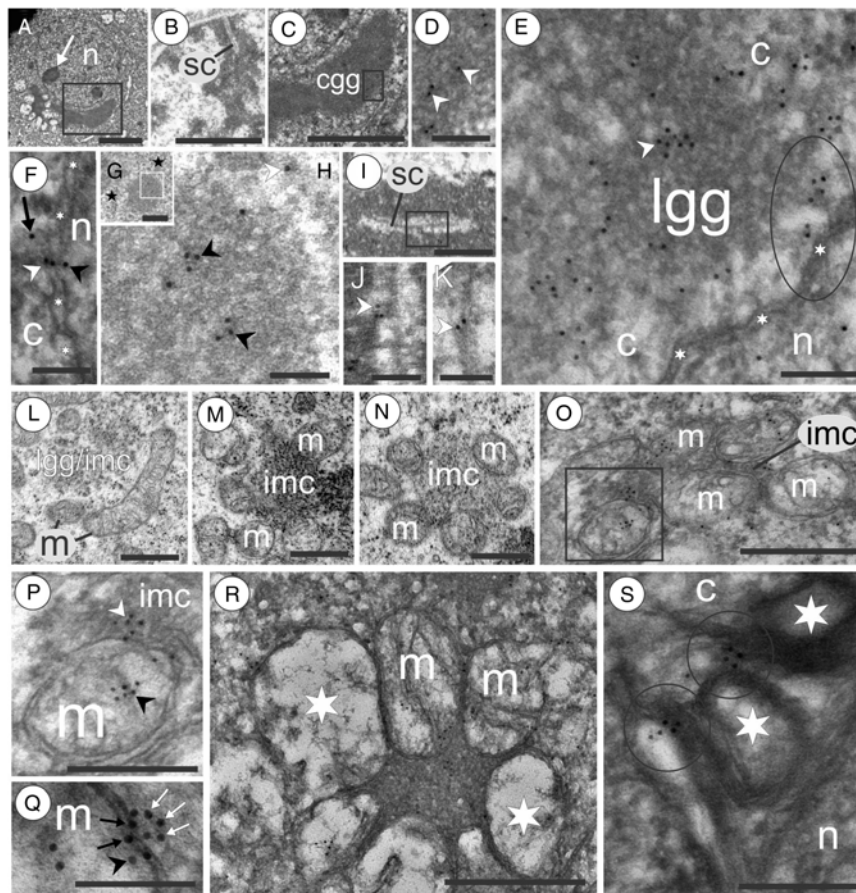


Figure 2. Patterns of GPRS in pre-zygotene–pachytene spermatogenesis of the marine medaka *O. melastigma*. (A) Spermatogonium identified by the presence of nucleoli (arrow) in the nucleus (n). Square is area magnified in (C, D). (B) Zygotene–pachytene spermatocyte identified by the presence of synaptonemal complexes (sc) in the nuclei. (C) Magnification of the area with compact germ plasm granule (cgg) outlined by the square in (C); note that the compact germ plasm granule is positive for Vasa (arrowheads). (D) Magnification of a compact germ plasm granule (cgg) outlined by the square in (C); note that the compact germ plasm granule is positive for Vasa (arrowheads). (E) Loosened germ plasm granule (lgg) that is located in the cytoplasm (c) and is positive for Vasa (arrowhead); note that the Vasa-positive strand of lgg contacts the membrane (asterisks) of the nucleus (n) as outlined by the ellipse. (F) Cytoplasmic Vasa (arrow) is found in the close vicinity to the nuclear membrane (indicated by asterisks), inside nuclear membrane (white arrowhead), and inside the nucleus (black arrowhead). (G) Nucleolus of spermatogonium; the square outlines the area magnified in (H); stars indicate nuclear chromatin. (H) Magnification of the nucleolus shown in (G); note that Vasa is located near (white arrowhead) and inside (black arrowheads) the nucleolus. (I) Synaptonemal complex (sc) of zygotene–pachytene spermatocyte; the square outlines the area magnified in (J). (J) Magnification of the area outlined by the square in (I); note Vasa (arrowhead) in the light periphery of synaptonemal complex. (K) Vasa (arrowhead) located immediately on the synaptonemal complex stripe. (L) Loosened germ plasm granule that became intermitochondrial cement (lgg/imc) as it contacted the mitochondria (m). (M) Intermitochondrial cement (imc) collared by four mitochondria (m). (N) IMC collared by five mitochondria (m). (O) Mature mitochondrial cluster with mitochondria (m) profoundly introduced into the IMC and closely attached to each other; the square outlines the area magnified in (P). (P) Magnification of the area outlined by the square in (O); note the Vasa (white arrowhead) located in the IMC and the Vasa (black arrowhead) located inside a mitochondrion (m). (Q) Vasa (white arrows) located near membranes of a mitochondrion (m) is situated between membranes (black arrows) and takes place in the vicinity of the inner membrane inside mitochondria (arrowhead). (R) Partly degraded mitochondrial cluster with both mitochondria with intact structures (m) and autolyzed mitochondria (asterisks). (S) Degraded mitochondrial clusters consisting of mitochondrial remnants (asterisks); note Vasa (shown by circles) seen between mitochondrial remnants; (c) cytoplasm, (n) nucleus. Scale bars = 1 μm (A–C), 0.2 μm (D–K), 0.5 μm (L–O, P, R, S), 0.1 μm (Q).

(Fig. 4D). Using immunohistology, we found that these cells had no any bright Vasa signal (Fig. 4C,D).

A spermatid is a cell with a head having some cytoplasm, a round nucleus containing chromatin strands, and a mitochondrial area (Fig. 5A). A cross-section through the mitochondrial area shows eight mitochondria located around the basal body of a flagellum (Fig. 5B). Both the anterior–posterior section through the spermatid head and the cross-section through the spermatid mitochondrial area showed the presence of an electron-dense chromatoid body in the mitochondrial area. This body was never found in contact with mitochondria (Fig. 5A,B). iEM at higher magnification showed that the chromatoid body was Vasa-positive and normally had a Vasa-positive diffused periphery (Fig. 5C). In late spermatids the Vasa was found in the cytoplasm of

mitochondrial area (Fig. 5D,E). Also, Vasa-positive matter was found in close contact with mitochondria (Fig. 5D,F) and inside mitochondria (Fig. 4D,G).

A spermatozoon is a flagellated cell with a nucleus filled with condensed electron-dense chromatin and a mitochondrial area (Fig. 5H). Cross-sections show that the Vasa-positive chromatoid body, which is characteristic for mitochondrial areas of spermatids, was absent in mitochondrial areas of sperm cells (Fig. 5I). iEM showed that some Vasa-positive matter could be rarely found in the cytoplasm of the mitochondrial area and in close contact with mitochondria (Fig. 5J,K). During observation, in both cross-sections and anterior–posterior sections of mitochondrial areas, no Vasa was found inside the mitochondria (Fig. 5L).

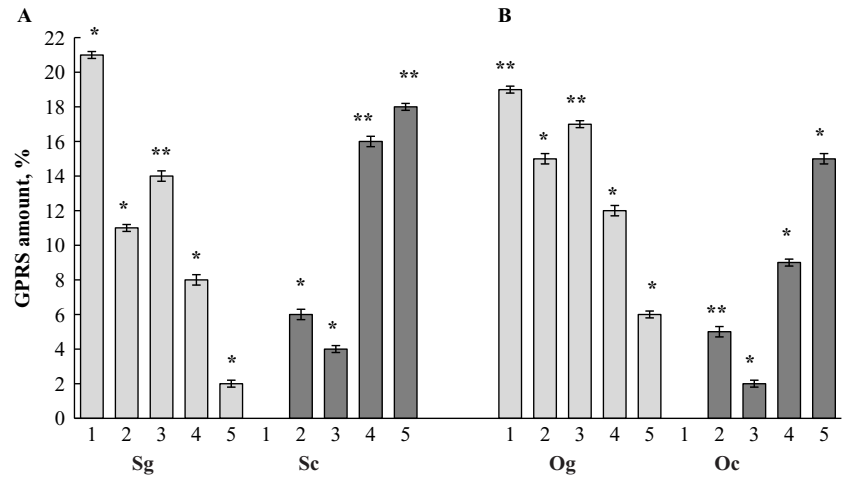


Figure 3. Dynamic of GPRS amounts observed during the mitosis-to-meiosis shift occurring in male (A) and female (B) germ cells of the marine medaka *O. melastigma*. Spermatogonia (sg), zygotene/pachytene spermatocytes (sc), oogonia (og), zygotene/pachytene oocytes (Oc). 1, compact germ plasm granule; 2, loosened germ plasm granule; 3, 'mitochondrial cluster'; 4, 'partly degraded mitochondrial clusters'; 5, 'degraded mitochondrial clusters'. Value is the mean \pm SEM for cells of each germ-cell types from females and males. GPRS quantities are statistically different (* $P < 0.05$; ** $P < 0.001$).

GPRS in pre-zygotene/pachytene oogenesis

Anti-Vasa antibodies were investigated by western blot for the marine medaka ovaries. The assay showed that the blot was quite accentuated for the ovaries. Blots ran at the level equivalent to 75 kDa (Fig. 1B).

As shown by immunohistology, the early oogenic cells were characterized by very dense Vasa staining (Fig. 4E). We identified oogonia at thin sections using such traits as the nuclei filled with granular chromatin and having nucleoli (Fig. 6A). To study zygotene–pachytene oocytes we looked for early oogenic cells that lacked nucleolus in their nuclei and showed the condensed chromatin strands with synaptonemal complexes (Fig. 6B). Both the oogonia and zygotene–pachytene oocytes had compact GG that were positive for Vasa, as shown by iEM (Fig. 6A,C,D) and loosened Vasa-positive GG were found in oogonia and oocytes (Fig. 6E). Quantitative analysis revealed that the proportions of GG patterns varied. In oogonia, compact GG constituted 19.0%; loosened GG, 15.0%. Zygotene–pachytene oocytes had no compact GG, but loosened GG accounted for 5.0% (Fig. 3B).

In both the oogonia and zygotene–pachytene oocytes, the Vasa-positive substance of loosened GG tended to contact the nucleus (Fig. 6E). Colloidal gold particles corresponding to Vasa protein were frequently found inside the nuclear membrane (nuclear pores) (Fig. 6G,F). Enlargement of oogonium nucleolus indicated that Vasa was located near and inside the nucleolus (Fig. 6G,H). In zygotene–pachytene oocytes, the Vasa was also found all over the nucleus and in the synaptonemal complexes (Fig. 6I).

The oogonia and zygotene–pachytene oocytes had mitochondrial clusters in the cytoplasm (Fig. 6A). These were routinely formed by loosened Vasa-positive GG playing a role in IMC that attached to mitochondria individually (Fig. 6J), and also appeared as a central core of clusters consisting of several mitochondria (Fig. 6K). Vasa was located in the IMC and inside mitochondria contacting the IMC (Fig. 6L).

Some clustered mitochondria were regularly found at various stages of degradation. Some mitochondria completely lacked their structures and contained electron-light cavities (Fig. 6K). Similar to spermatogenic cells, some clusters were totally degraded (not shown). Quantitative analysis showed that proportions of mitochondrial cluster types varied. In oogonia, the mitochondrial clusters consisted of 17.0% MC, 12.0% PDMC and 6.0% DMC.

Zygotene–pachytene oocytes contained fewer MC (2.0%). However, there were more PDMC and DMC, constituting 9.0% and 15.0%, respectively (Fig. 3B).

GPRS in post-zygotene/pachytene oogenesis

As is found in histologic sections of the ovary, germline cells were represented by various stages of oocyte growth (Fig. 7A). To study GPRS, we selected five stages of advanced oogenesis according to cell size increases (Fig. 4F–J).

As shown by immunohistology, growing oocyte 1 and growing oocyte 2 were distinguished by a perinuclear Vasa-positive layer (Fig. 4F,G). The larger magnification obtained by electron microscopy confirmed that Vasa were present in the perinuclear layer (Fig. 7B,C); also it was found that Vasa was located near the nuclear membrane (Fig. 7B,D) and inside the nucleus (Fig. 7B,E). The perinuclear layers of both the growing oocytes 1 and the growing oocytes 2 contain GG that were positive for Vasa in both the central compact area and the diffused periphery (Fig. 7F). Some GG were remote from the nucleus (Fig. 7G), some were located near the nucleus (Fig. 7H), and some were found in direct contact with the nucleus (Fig. 7I). Some GG contacting the nucleus played a role in IMC that aggregated mitochondria into clusters. Mitochondrial clusters were found in direct contact with the nucleus in both growing oocyte 1 (Fig. 7G) and the growing oocyte 2 (Fig. 7J). In the mitochondrial clusters, Vasa was found inside both the IMC and the mitochondria (Fig. 7K). Growing oocyte 3 lacked a perinuclear Vasa-positive layer, although some diffused Vasa signal registered in the cytoplasm (Fig. 4H). No GG, IMC, and MC were found using electron microscopy, despite the scrupulous examination of serial sections (Fig. 7L).

The growing oocytes were surrounded by a follicular envelope undergoing progressive enlargement. In growing oocytes 1–3, this envelope has no clear Vasa signal (Fig. 4F–H). In growing oocyte 4 (vitellogenic oocytes), there were Vasa-positive structures with intense staining (Fig. 4I). The follicular envelope of oogenesis stage 5 (late vitellogenic oocytes) had a more faint Vasa signal (Fig. 4J). Using electron microscopy, we observed the dynamics of follicular envelope cell progression. It was characteristic that electron-light vacuoles were present in the follicle cells (Fig. 8A). These vacuoles appeared due to amalgamation of some mitochondria (Fig. 8B). The completely formed vacuoles

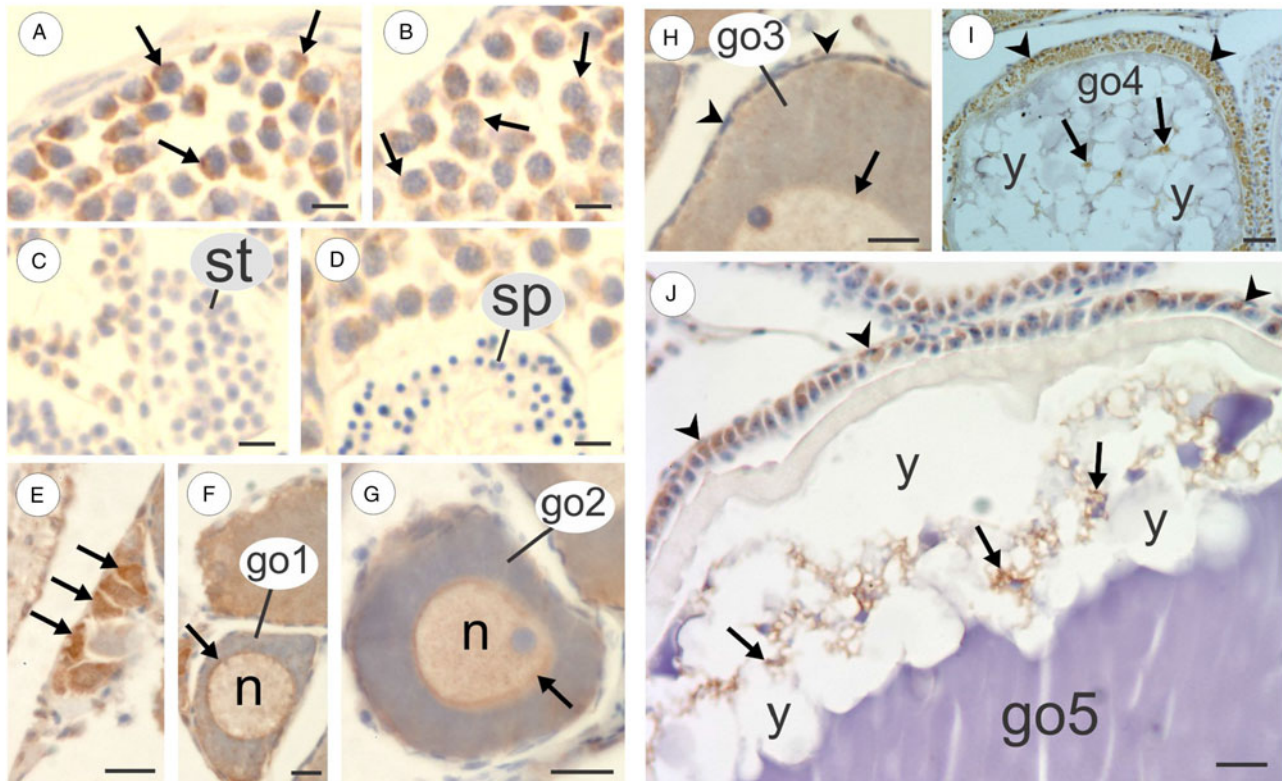


Figure 4. Vasa protein expression during spermatogenesis (A–D) and oogenesis (E–J) of marine medaka *O. melastigma* by immunohistochemistry. Gonadal sections were stained with Vasa antibody (brown). For spermatogenesis, staining was analyzed in: (A) spermatogonia (B), primary spermatocytes, (C) spermatids and (D) spermatozoa. The signal was most intense and appeared non-central in spermatogonia (A, arrows); it appeared weaker, as well as obtained uniform localization, in spermatocytes (B, arrows); and was almost absent in spermatids (C, st) and spermatozoa (D, sp). For oogenesis, the staining was analyzed in: (E) oogonia that are characterized by having an intense Vasa signal (arrows); (F) growing oocytes 1 (go1); and (G) growing oocytes 2 (go2) that have an intense Vasa signal (arrows in F, G) around the nucleus ('n' in F, G); (H) growing oocytes 3 (go3) that lacks the Vasa signal in the perinuclear area (H, arrow) and have no Vasa signal in the follicle envelope (arrowheads); (I) stage 4 growing vitellogenic oocyte (go4) that has the Vasa-positive follicle envelope (arrowheads), and Vasa is also located (arrows) between yolk granules (y); (J) stage-5 late vitellogenic oocyte (go5) that had a weaker Vasa signal in its follicle envelope (arrowheads), and Vasa was also located (arrows) between yolk granules (y). Scale bars = 10 µm.

normally contained granules with an elongated (Fig. 8C) or round shape (Fig. 8D). The vacuole was filled by a diffused Vasa-positive substance (Fig. 8E). This substance was observed to be directly attached to the granule that was intensely stained with Vasa (Fig. 8F). The developed Vasa-positive granule was surrounded by membrane (Fig. 8G). Vasa-positive granules had an elongated shape and were often attached with their end to the oocyte membrane (Fig. 8H,I). In a cross-section it can be seen that granule bases were tightly assimilated with the oocyte membrane that usually had a wavy shape (Fig. 8J). Late stage 5 vitellogenic oocytes with formed chorion were surrounded by follicle cells that contained small amounts of granules. Granule remnants attached to the oocyte envelope could be rarely found (Fig. 8K).

In the stage 4 vitellogenic oocytes and stage 5 late vitellogenic oocytes, Vasa-positive granules had an external layer that was similar in colour and texture to the developing egg chorion, and the granule amalgamate with the chorion by this external layer (Fig. 9A). Magnification of Fig. 9(A) showed that Vasa is present in the vicinity of the oocyte membrane, on the oocyte membrane, and in the oocyte cytoplasm immediately after the oocyte membrane (Fig. 9B). In late oocytes with developed chorion, Vasa was not found in the chorion substance but was frequently found in the microvilli located in the chorion channels (Fig. 9C,D). The growing oocyte 4 and late-stage 5 vitellogenic oocytes normally had a concentrated Vasa signal between yolk aggregations. The areas of Vasa locations were rather remote from the oocyte envelope (Fig. 4I,J). By iEM, it

was found that Vasa aggregations were located in the electron-dense substance with an amorphous shape (Fig. 9E–G).

Discussion

GPRS transformation during mitosis-to-meiosis shift is similar in both sexes

One of the aims of this study was to investigate GPRS activity occurring during mitosis-to-meiosis shift in female and male gonads. In fish including marine medaka, premeiotic gonial cell differentiation typically includes several generations (Leal *et al.*, 2009; Schulz *et al.*, 2010; Lacerda *et al.*, 2014). To optimize the study, we used ultrastructural criteria that allowed reliable comparative analysis of premeiotic cells and cells entering early meiosis. According to some reports summarizing ultrastructural features of metazoan meiotic cells, the premeiotic female cells (oogonia) and the premeiotic male cells (spermatogonia) were ultrastructurally similar and had a nucleolus in their dispersed chromatin. Early female meiotic cells (oocyte 1) and early male meiotic cells (spermatocyte 1) were distinguished by chromatin condensation and appearance of distinctive synaptonemal complexes of synapsed chromosomes when chromosomal crossing-over occurred at the zygotene–pachytene stage of meiosis (Eckelbarger, 2005; Ables, 2015). Therefore, thanks to the existence of ultrastructural criteria that allowed discrimination of premeiotic and early meiotic cells, it was technically possible

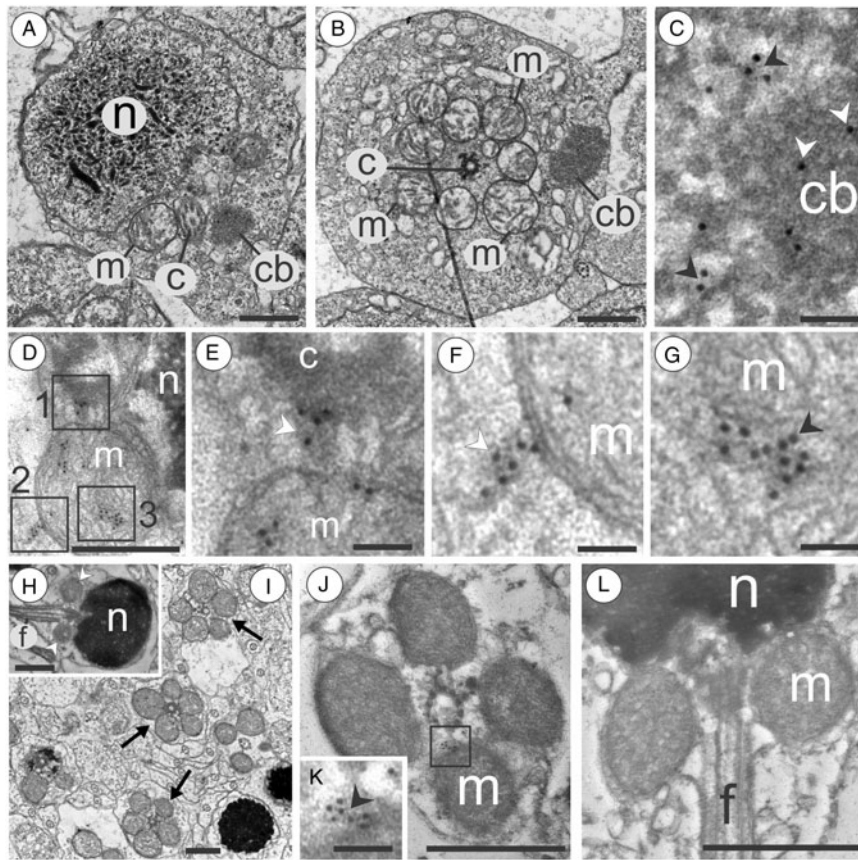


Figure 5. Patterns of GPRS in spermatids and sperms of the marine medaka *O. melastigma*. (A, B) Longitudinal sections (A) and cross-sections (B) through the mitochondrial area of the spermatid that is peculiar in having a nucleus (n), centriole (c), mitochondrion (m) and chromatoid body (cb). (C) Chromatoid body (cb) that is positive for Vasa (white arrowheads) in its central area and in its diffused periphery (black arrowheads). (D–G) Mitochondrial area (D) of late spermatid; magnification (E) of the square 1 in (D) shows that Vasa (arrowhead) is located between the centriole (c) and mitochondrion (m); magnification (F) of the square 2 in (D) and shows that Vasa-positive substance (arrowhead) contacts a mitochondrion (m); magnification (G) of the square 3 in (D) shows that Vasa (arrowhead) is located inside a mitochondrion (m). (H) Longitudinal section through a spermatozoon that consists of a nucleus (n), mitochondrial area (arrowheads), and flagellum (f). (I) Cross-sections through mitochondrial areas (arrows) show that chromatoid body is absent in sperm cells. (J) Cross-section through mitochondrial areas of sperms. Magnification (K) of the square shown in (J) detects that Vasa (arrowhead) is located by mitochondrion (m). (L) Longitudinal section through a spermatozoon that is negative for Vasa; n, nucleus; m, mitochondrion; f, flagellum. Scale bars = 0.5 μm (A, B, D, H, J, L), 0.1 μm (C, E, F, G, K).

to make a comparison of GPRS transformation occurring during the mitosis-to-meiosis shift.

It has been reported that fish oögonia and spermatogonia were ultrastructurally similar in both sexes (Sato, 1974; Billard, 1984; Flores and Burns, 1993; Braat *et al.*, 1999). Our data have confirmed that in marine medaka the female and male gonial cells (oögonia and spermatogonia) were ultrastructurally similar in having nucleoli in the nuclei. Also, in both sexes the zygotene–pachytene meiotic cells were similar in having synaptonemal complexes. In both females and males, premeiotic and meiotic cells had a Vasa-positive compact GG (Fig. 10A,G).

We found that the ‘yellow phase’ of meiosis was similar in males (10A–C) and females (Fig. 10G–I). It was characterized by the presence of compact Vasa-positive GG. However, some Vasa-positive GG appeared in a loosened shape. As the amount of compact GG was dominant in spermatogonia and oögonia but greatly decreased during differentiation into the zygotene–pachytene spermatocytes and corresponding oocytes, it seems logical that compact granules were reduced in number during the mitosis-to-meiosis shift. Taking into account that loosened germ plasma granules dominated in the zygotene–pachytene meiotic cells of both sexes, we suggested dispersion of compact GG to the loosened form that occurred during the onset of meiosis (Fig. 10A,B,G,H). Our quantification analysis also showed that the total amount of Vasa-positive GG

with both compact and loosened forms dramatically decrease during the mitosis-to-meiosis shift, assuming fast consumption of Vasa-positive substances. This observation allowed the suggestion on a role for Vasa-positive GG in the mitosis-to-meiosis shift.

We found that in marine medaka the loosened GG undergo dispersion in the cytoplasm and form Vasa-positive strands attaching to the nucleus. Vasa-labelling was also found in the nuclear membrane pores and inside the nuclei. In the gonial cells of both sexes, a Vasa signal was registered in nucleoli (Fig. 10B,H). In the male and female zygotene–pachytene cells, Vasa was regularly found in the synaptonemal complex (Fig. 10C,I). It is worth noting that the presence of Vasa both in the cytoplasm and nucleus was also reported for oocytes of *Drosophila* (Findley *et al.*, 2003). Pek and Kai (2011) reported the perichromosomal localization of Vasa and its role in *Drosophila* mitotic chromosome condensation. Based on these findings and our present observation, we suggest that Vasa participates in a kind of premeiotic chromatin reorganization.

It was also observed that the loosened form of GG formed mitochondrial clusters (Fig. 10B, H) obviously acting as the so-called IMC that usually agglutinates mitochondria in reproductive cells (see review in Chuma *et al.*, 2009). We noticed that mitochondria cemented with IMC underwent degradation. By quantification of the intact mitochondrial clusters, PDMC, and DMC, we observed that degradation of clustered mitochondria normally occurred

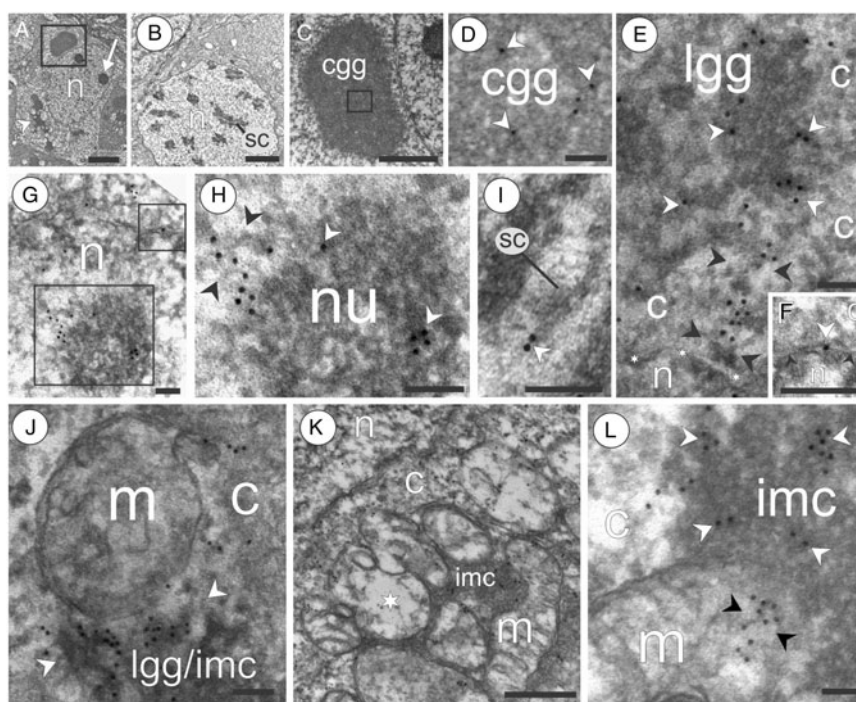


Figure 6. Patterns of GPRS in pre-zygotene–pachytene oogenesis of the marine medaka *O. melastigma*. (A) Oogonium that is identified by the presence of nucleoli (arrow) in the nuclei; arrowhead indicates mitochondrial cluster; the square outlines the area magnified in (C). (B) Zygotene–pachytene oocyte identified by the presence of synaptonemal complexes (sc) in the nucleus (n). (C) Magnification of the area with compact germ plasm granule (cgg) outlined by the square in (A). (D) Magnification of compact germ plasm granule (cgg) outlined by the square in (C); note that the compact germ plasm granule is positive for Vasa (arrowheads). (E) Loosened germ plasm granule (lgg) that is located in the cytoplasm (c) and positive for Vasa (white arrowheads); note a Vasa-positive strand (indicated by black arrowheads) contact nucleus (n); nuclear membrane is indicated by asterisks). (F) Magnification of the area outlined by the small square in (E); note Vasa (white arrowhead) found inside nuclear membrane (indicated by black arrowheads). (G) Nucleus (n) of oogonium; note the area of nuclear membrane (small square) magnified in (F) and a nucleolus (large square). (H) Magnification of nucleolus (nu) shown in (G); note the Vasa located in the vicinity (black arrowheads) of the nucleolus and Vasa (white arrowheads) inside the nucleolus. (I) Vasa (arrowhead) inside a synaptonemal complex (sc). (J) Loosened germ plasm granule that is positive for Vasa and performed the role of intermitochondrial cement (lgg/imc) that tended to contact a mitochondrion (m); note the area of contact between the mitochondrion and the intermitochondrial cement (indicated by arrowheads). (K) Mature mitochondrial cluster with mitochondria (m) that are profoundly introduced into the intermitochondrial cement (imc) and closely attached to each other; note a mitochondrion with an autolyzed content (asterisk). (L) IMC that is positive for Vasa (white arrowheads) and contacts a mitochondrion (m); note Vasa (black arrowheads) that is inside a mitochondrion; c, cytoplasm; n, nucleus. Scale bars = 1 μ m (A, B), 0.5 μ m (C, K), 0.1 μ m (D–J, L).

during the mitosis-to-meiosis shift in both sexes (Fig. 10C,I). It seems logical that the appearance of degraded mitochondria completes the cascade of interactions between GG and mitochondria. Previously, premeiotic disassembly of mitochondria induced by the GG substance has been described in some species (Reunov *et al.*, 2000). This fact may help understanding the mechanism of extramitochondrial localization of mitochondrial ribosomes during gametogenesis (Villegas *et al.*, 2002). Amikura *et al.*, (2005, 2001), as well as Gur and Breitbart (2006, 2008), suggested that mitochondrial ribosomes could translate nuclear RNAs during germline cells differentiation. Our study showed that in mitochondrial clusters Vasa was found in contact with some mitochondria and inside mitochondria (Fig. 10B,C,H,I). We noticed that Vasa penetration in mitochondria anticipated mitochondria destruction. Therefore, a role for Vasa in premeiotic mitochondrial degradation could be supposed.

Chromatoid body is an accessory structure specific to postmeiotic spermatogenesis

Spermatids of marine medaka contained a Vasa-positive structure that was morphologically similar to an analogous structure routinely described as a ‘chromatoid body’ (CB). Initially, Fawcett (1972) reported that in rat spermatids the CB arose as a stock of mRNAs formed due to the conservation of the nuclear

genome and directed towards translation of proteins essential for the sperm tail formation rather than having any importance for the early stages of meiosis. Indeed, as was shown, the CB was a centre of RNA synthesis during the late stages of spermiogenesis, a stage characterized by low RNA synthesis over the entire cell (see review in Onohara and Yokota, 2012). It has been reported that the CB contains testis-specific serine/threonine kinases and forms ring-shaped structures around a mitochondrial sheath; deletion of required genes resulted in the loss of chromatoid body-derived rings and the collapse of the mitochondrial sheath (Shang *et al.*, 2010). It was speculated (Meikar *et al.*, 2011) that, although the CB in mouse and the GG in lower organisms (fly, nematode, or frog) share many protein components, these granules and CB apparently supported different biological functions. Some data are available on the localization of proteins such as Ago2, Ago3, Dcp1a and GW182, which are the routinely used as markers for the processing body (P-body), granules that are responsible for RNA silencing and RNA disruption in somatic cells. This allows speculation that the CB may be functionally comparable with P-bodies (see review in Chuma *et al.*, 2009; Onohara and Yokota, 2012). Therefore, it seems possible that the CB does not belong to GG promoting meiotic differentiation, but more likely is a highly specialized granule characteristic of the final stage of sperm formation in some species. Actually, CB has been found in spermatids of a limited group of vertebrate animals (see review

Figure 7. Patterns of GPRS in advanced oogenesis of the marine medaka *O. melastigma*. (A) Histological section shows that adult ovary is filled by oocytes at various stages of growth. (B) Growing oocyte 1 with areas outlined by squares in perinuclear layer (square 1), nuclear membrane (square 2), and nucleus (square 3). (C–E) Magnifications of the areas outlined by squares 1, 2 and 3, respectively, in (B); note Vasa (arrowheads) in the perinuclear area (C), near the nuclear membrane (indicated by asterisks) (D), and inside the nucleus (E). (F) Germ plasma granules positive for Vasa in its compact central area (white arrowheads); note Vasa (black arrowheads) in the diffused periphery of the germ plasma granule. (G) Growing oocyte 1; a sample of germ plasma granule (showed by arrow) remote from the nucleus; note a mitochondrial cluster (outlined by circle) located in close contact with the nucleus. (H) Sample of germ plasma granule (indicated by arrow) located near the nucleus. (I) Sample of germ plasma granule (outlined by circle) located in direct contact with the nucleus. (J) Growing oocyte 2: a mitochondrial cluster consisting of mitochondria (m) agglutinated by intermitochondrial cement (imc); note that mitochondrial cluster in a close contact with the nucleus. (K) IMC that is positive for Vasa (white arrowheads) and contacts a mitochondrion (m); note Vasa (black arrowheads) inside a mitochondrion. (L) Growing oocyte 3; note a perinuclear layer (arrowheads) that lacks germ plasma granules and mitochondrial clusters; n, nucleus; c, cytoplasm. Scale bars = 30 μ m (A), 0.1 μ m (B–F, K), 0.5 μ m (G–J, L).

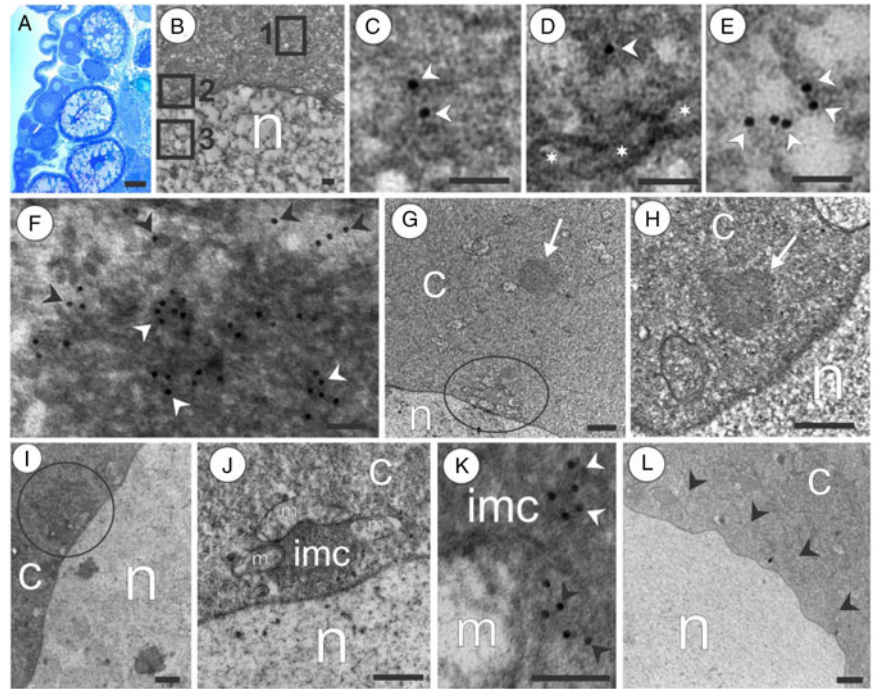
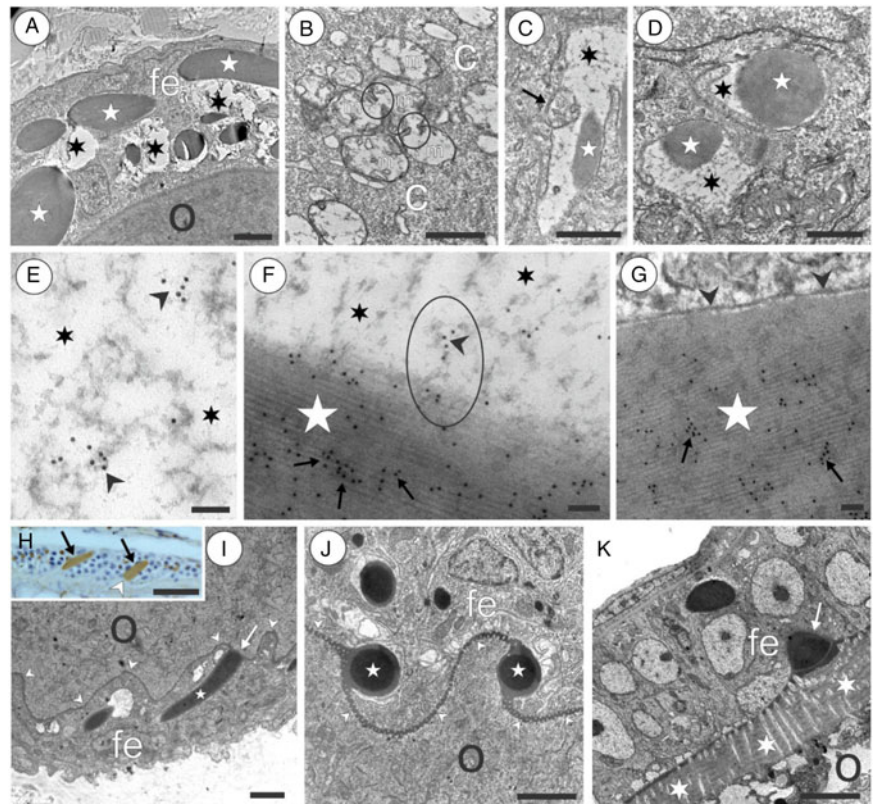


Figure 8. Vasa-positive granules in the follicular envelope of oocytes in the marine medaka *O. melastigma*. (A) Oocyte (o) surrounded by a follicular envelope (fe); note vacuoles (asterisks) present in the cytoplasm of follicular cells. (B) Group of mitochondria (m) in the cytoplasm (c) of follicular cells; note junctions (outlined by circles) that connect some mitochondria. (C) A vacuole (asterisk) that arose by amalgamation of mitochondria; it contains an elongated electron-dense granule (star); note a mitochondrion located at the periphery of a vacuole (arrow). (D) Vacuoles (asterisks) containing electron-dense granules with a round shape (stars). (E) Vacuole space (asterisks) filled by a substance with a signal for Vasa (arrowheads). (F) Vacuole space (asterisks) with developing electron-dense granules (star) positive for Vasa in its central area (arrows); note the ellipse outlining a substance strand that is positive for Vasa (black arrowhead) and contacts a Vasa-positive electron-dense granule. (G) Formed electron-dense granule (star) that is positive for Vasa (arrows) and is surrounded by a membrane (arrowheads). (H) Oocyte periphery visualized by immunohistochemistry; note the formed Vasa-positive granules (brown) that have an elongated shape (arrows) and contact with the oocyte membrane (arrowhead). (I) Electron-dense granule (star) attached to the oocyte membrane (arrowheads) with its end (arrow). (J) Cross-section shows that granule bases (asterisks) are tightly assimilated with the oocyte membrane that usually has a wavy shape (arrowheads). (K) Maturing oocyte separated from the follicle envelop (fe) by the modified oocyte membrane (asterisks); note a granule remnant (arrow); fe, follicle envelope, o, oocyte. Scale bars = 0.5 μ m (A–D, I–K), 0.1 μ m (E–G), 10 μ m (H).



in Kalt, 1973; Kerr and Dixon, 1974; Eddy, 1975). However, there are examples showing that CB is absent during spermatogenesis although the GG, IMC, and mitochondrial clusters are normally present during early meiosis. CB were not detected in spermatogenesis of sipunculids (Reunov and Rice, 1993), nemerteans

(Reunov and Klepal, 1997), polychaetes (Reunov *et al.*, 2010), bivalve molluscs (Reunov *et al.*, 2018), phoronids (Reunov and Klepal, 2004), brachiopods (Hodgson and Reunov, 1994), and echinoderms (Au *et al.*, 1998). Therefore, in the animal kingdom there are two patterns of spermatogenesis that are uniform

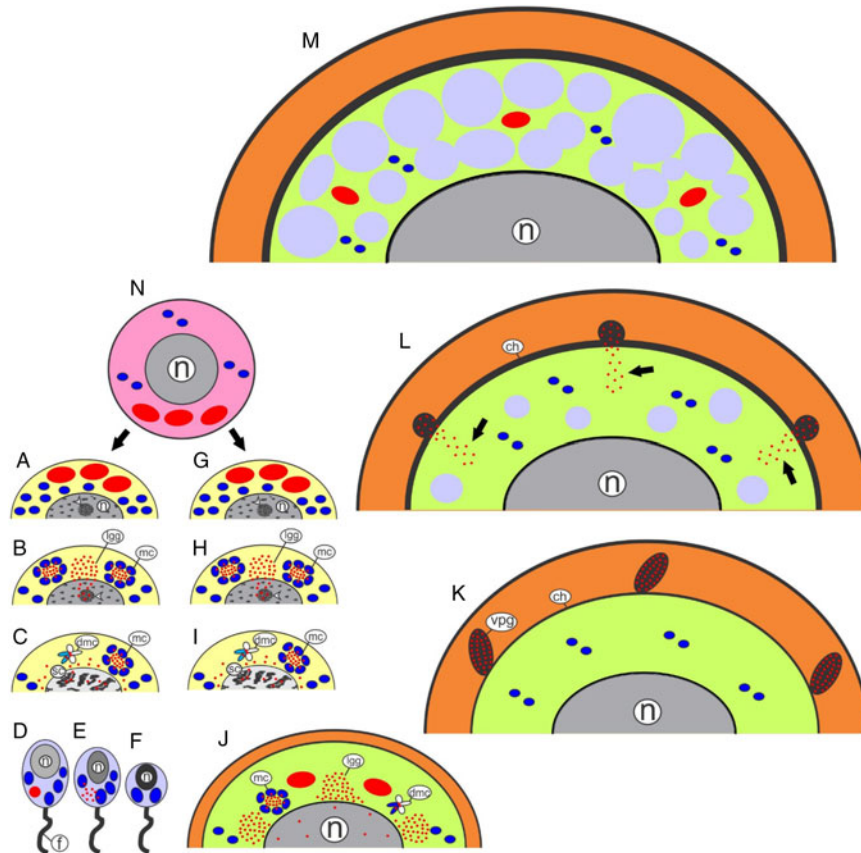


Figure 10. Schematic drawing of GPRS dynamics in the meiotic differentiation of males (A–F) and females (G–M) of the marine medaka *O. melastigma*. Note that ‘yellow phase’ of meiosis is similar in males (A–C) and females (G–I) and is characterized by the presence of compact Vasa-positive germ plasm granules (red) that are unrelated to mitochondria (blue); any Vasa is not present in the cytoplasm and nucleolus (arrowheads) of nuclei (n) (A, G); germ plasm granule transformation to the loosened germ plasm granules (lgg), followed by penetration of this Vasa-positive loosened fraction (red dots) to the nuclei with localization in the nucleolus (arrowheads) of spermatogonia and oogonia (B, H); transformation of some of this fraction into the intermitochondrial cement (red dots) aggregating neighbouring mitochondria (blue) to mitochondrial clusters (mc) (B, H). Note that in zygotene–pachytene meiotic cells some Vasa (red dots) is present in synaptonemal complexes (sc); degraded mitochondrial clusters (dmc) coexist with intact mitochondrial clusters (mc) (C, I). Advanced spermatogenesis (spermiogenesis) is characterized by arising of a chromatin body (red) that is unrelated to mitochondria in early spermatids (blue) (D) and undergoes dissemination followed by the Vasa-positive substance (red dots) penetration into some mitochondria (blue) in the middle spermatids (E). Note the complete absence of Vasa in the sperm (F). Growing oocytes 1 and 2 are distinguished by newly arisen compact germ plasm granules (red), loosened germ plasm granules (lgg), mitochondrial clusters (mc), and degraded mitochondrial clusters (dmc); note some Vasa (red dots) in the nucleus (n) (J). Growing oocytes 3 lack any GPRS in the cytoplasm (green), but Vasa-positive granules (vpg) arise in cells of follicle envelope (brown) and attached to the chorion (ch) (K). Subsequently the process continues with injection of Vasa from the Vasa-positive granules through the chorion (ch) to the cytoplasm (Vasa is indicated by arrows) (L) and storage of Vasa-positive germ plasm granules (red) between yolk aggregations (light grey colour) (M); note that nuclei (n) do not contain Vasa and mitochondria (blue) do not contact any germ plasm structures in late oocytes (K–M). During embryo development, the compact germ plasm granules (red) formed in late oocytes (M) are inherited by primordial germ line cells (pink) giving rise to meiotic lines of both sexes (arrows) (N); f, flagellum; n, nucleus.

to as ‘follicle cell assigned germ plasm formation’. This mechanism describes the process that appears morphologically different compared with the Balbiani body (= mitochondrial cloud) which is usually associated with the GG formation (Kalt, 1973; Kloc *et al.*, 2002; Cox and Spradling, 2003; Chang *et al.*, 2004; Wilk *et al.*, 2004). We did not find any Balbiani body in the oocytes. It seems likely that the Balbiani body is absent in medaka, and we discovered an original type of GG formation. It was shown that the process was started by aggregation of some mitochondria in the cytoplasm of follicular cells (Fig. 11A,B). Mitochondria swell and merge together to form a vacuole (Fig. 11C). Then the process continues with the appearance of diffused Vasa-positive substances in the vacuole followed by gradually growing Vasa-positive granules (Fig. 11D–F). The process progresses by attachment of Vasa-positive granules to the oocyte chorion (Fig. 10K) and Vasa injection through the chorion (Fig. 10L). It is noteworthy that, apart from Vasa delivery to the cytoplasm, the granules

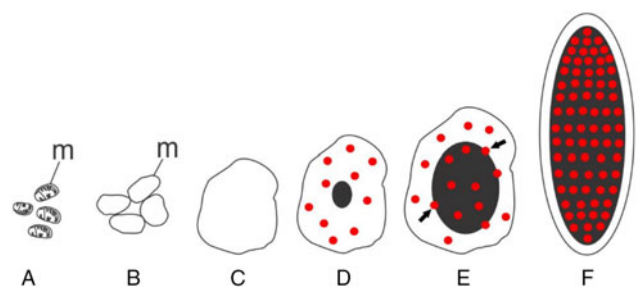


Figure 11. Schematic drawing of the progressive stages of Vasa-positive granule formation occurring in oocyte follicle cells of the marine medaka *O. melastigma*. During Vasa-positive granules formation, the mitochondria (A) swell and merge together (B) to form a vacuole (C). Then the process continues with the appearance of diffused Vasa-positive substances in the vacuole (D, red) followed by the arising of gradually growing granule (black) that takes up Vasa (D–F); m, mitochondria; arrows indicate the areas of Vasa (red) penetration into the granule (E).

contributed to enlargement of the growing oocyte envelope. We noticed that thickening of the oocyte chorion was accompanied with a shift from simple Vasa diffusion to Vasa transportation through microvilli penetrating the chorion. According to our data, the diffused Vasa spreads throughout the oocyte cytoplasm. In late-stage 5 vitellogenic oocytes we found GG-like bodies located between yolk accumulations (Fig. 10M). We did not find any special mechanism of formation of these bodies and suggested that GG were formed by condensation of the Vasa-positive substance. It seems very possible that these are storing GG following a preformative way of germ plasm inheritance, a mechanism previously supposed for teleost fish (Hamaguchi, 1982, 1985; Timmermans and Taverne, 1989; Braat *et al.*, 1999; Knaut *et al.*, 2000). This mechanism assumes the early segregation of Vasa-positive GG in late oocytes and their localization in PGC during embryogenesis (Fig. 10N).

Conclusions

In the present study of both sexes' gametogenesis in the marine medaka *Oryzias melastigma*, we investigated GPRS during the mitosis-to-meiosis period, post-zygotene/pachytene period, and during their deposition in oogenesis.

Using anti-Vasa antibodies (germ plasm marker) and based on ultrastructural analysis, we found that premeiotic GPRS transformation was not sex specific. In both sexes, a shift from mitosis to meiosis was characterized by the following steps: (1) turning of Vasa-positive GG into IMC; (2) formation of mitochondrial clusters due to the agglutinating effect of IMC; and (3) entry of the IMC-originated Vasa-positive substance into clustered mitochondria; followed by (4) structural demolishing of clustered mitochondria that may correspond to the cytoplasmic localization of mitochondrial ribosomes, as previously described in germ cells of *Drosophila*, *Xenopus*, and mice; and (5) entry of Vasa-positive substance into the nucleus to promote, as suggested, meiotic remodelling of chromatin during the mitosis-to-meiosis shift.

The post-zygotene/pachytene period is sex specific, assuming CB appearing in spermatogenesis and GG-like structures in oogenesis; in both sexes these are accessory structures probably serve to extend the release of mitochondrial matter.

A new type of GG arising, 'the follicle cell assigned germ plasm formation', was discovered in oogenesis of marine medaka.

Recommendations concerning artificial meiotic differentiation are made as follows: (1) presence of Vasa-positive GG is crucial for successful mitosis-to-meiosis shift in stem cells; the electron microscopy should be involved to sample GG presence/absence in stem cells targeted for meiotic differentiation; and (2) taking into account that the primary step of GG formation occurs in the oocyte follicle cells (FC), co-cultivation of FC together with stem cells may be considered if stem cells lack the inherited GG.

Acknowledgements. This study was supported by the Russian Programme for Basic Research 'The Far East' (project no. 15-I-6-007_o), and was partially funded by the CityU Strategic Research Grant (project no. 7005098) and the State Key Laboratory of Marine Pollution grant, CityU. The study was done using equipment of the State Key Laboratory of Marine Pollution, Department of Chemistry, City University of Hong Kong (Hong Kong), and electron microscopy facility of the National Scientific Center of Marine Biology (Vladivostok, Russia). A part of the study was done in the Microscopy Facility at St Francis Xavier University (Antigonish, NS, Canada).

Authors' contributions. AR designed the study, implemented most part of work by TEM and was a major contributor in writing the manuscript. DA designed the study and was a contributor in writing the manuscript. YNA

performed material collection/processing and some part of TEM analysis. MWLC performed material collection/processing, western blotting (WB) and light microscopy (LM) analysis. MTW performed material collection/fixation/processing, WB and LM analysis. KVY designed the antibody generation. YAR performed some part of TEM analysis with quantitative analysis. AVK performed some part of TEM analysis. NKMC performed fish maintenance, DRP performed fish collection, AVA was a contributor in discussion and writing the manuscript. All authors read and approved the final manuscript.

Conflicts of interest. We declare we have no competing interests.

Ethical standards. Animal maintenance and the experiments described below were reviewed and approved by the City University of Hong Kong Research Committee for its compliance with the Animals (Control of Experiments) Ordinance, Cap. 340, of the Hong Kong Special Administrative Region.

References

- Ables ET (2015) *Drosophila* oocytes as a model for understanding meiosis: an educational primer to accompany 'Corolla is a novel protein that contributes to the architecture of the synaptonemal complex of *Drosophila*'. *Genetics* **199**, 17–23.
- Amikura R, Kashikawa M, Nakamura A and Kobayashi S (2001) Presence of mitochondria-type ribosomes outside mitochondria in germ plasm of *Drosophila* embryos. *PNAS* **98**, 9133–8.
- Amikura R, Sato K and Kobayashi S (2005) Role of mitochondrial ribosome dependent translation in germline formation in *Drosophila* embryos. *Mech Dev* **122**, 1087–93.
- Au DWT, Reunov AA and Wu RSS (1998) Four lines of spermatid development and dimorphic spermatozoa in the sea urchin *Anthocidaris crassispina* (Echinodermata, Echinoidea). *Zoomorphology* **118**, 159–68.
- Billard R (1983) Spermiogenesis in the rainbow trout (*Salmo gairdneri*): An ultrastructural study. *Cell Tissue Res* **233**, 265–84.
- Billard R (1984) Ultrastructural changes in the spermatogonia and spermatocytes of *Poecilia reticulata* during spermatogenesis. *Cell Tissue Res* **237**, 219–26.
- Bontems F, Stein A, Marlow F, Lyautey J, Gupta T, Mullins MC and Dosch R (2009) Bucky ball organizes germ plasm assembly in zebrafish. *Curr Biol* **19**, 414–22.
- Braat AK, Speksnijder JE and Zivkovic D (1999) Germ line development in fishes. *Int J Dev Biol* **43**, 745–60.
- Carré D, Djediat C and Sardet C (2002). Formation of a large Vasa-positive germ granule and its inheritance by germ cells in the enigmatic chaetognaths. *Development* **129**, 661–70.
- Castrillon DH, Quade BJ, Wang TY, Quigley C and Crum CP (2000) The human VASA gene is specifically expressed in the germ cell lineage. *PNAS* **17**, 9585–90.
- Chang P, Torres J, Lewis RA, Mowry, KL, Houliston E and King ML (2004) Localization of RNAs to the mitochondrial cloud in *Xenopus* oocytes through entrapment and association with endoplasmic reticulum. *Mol Biol Cell* **15**, 4669–81.
- Chuma S, Hosokawa M, Tanaka T and Nakatsuji N (2009) Ultrastructural characterization of spermatogenesis and its evolutionary conservation in the germline: germinal granules in mammals. *Mol Cell Endocrinol* **306**, 17–23.
- Cox RT and Spradling AC (2003). A Balbiani body and the fusome mediate mitochondrial inheritance during *Drosophila* oogenesis. *Development* **130**, 1579–90.
- Eckelbarger KJ (2005). Oogenesis and oocytes. *Hydrobiologia* **535/536**, 179–98.
- Eddy EM (1975) Germ plasm and the differentiation of the germ cell line. *Int Rev Cytol* **43**, 229–80.
- Fawcett DW (1972) Observations on cell differentiation and organelle continuity in spermatogenesis. Proceeding of the Edinburgh Symposium. On the genetics of the spermatozoon. Bogtrykkeriet Forum. Copenhagen, pp. 37–68.
- Findley SD, Tamanaha M, Clegg NJ and Ruohola-Baker H (2003) *Maelstrom*, a *Drosophila* spindle-class gene, encodes a protein that colocalizes with Vasa and RDE1/AGO1 homolog, Aubergine, in nuage. *Development* **130**, 859–71.

- Flores JA and Burns JR (1993) Ultrastructural study of embryonic and early adult germ cells, and their support cells, in both sexes of *Xiphophorus* (Teleostei: Poeciliidae). *Cell Tissue Res* **271**, 263–70.
- Gur Y and Breitbart H (2006) Mammalian sperm translate nuclear-encoded proteins by mitochondrial-type ribosomes. *Genes Dev* **20**, 411–6.
- Gur Y and Breitbart H (2008) Protein synthesis in sperm: dialog between mitochondria and cytoplasm. *Mol Cell Endocrinol* **282**, 45–55.
- Gustafson EA and Wessel GM (2010) DEAD-box helicases: posttranslational regulation and function. *Biochem Biophys Res Commun* **395**, 1–6.
- Hamaguchi S (1982) A light and electron microscopic study of the migration of primordial germ cells in the teleost *Oryzias latipes*. *Cell Tissue Res* **227**, 139–51.
- Hamaguchi S (1985) Changes in the morphology of the germinal dense bodies in primordial germ cells of the teleost *Oryzias latipes*. *Cell Tiss Res* **240**, 669–73.
- Hartung O, Forbes MM and Marlow FL (2014) Zebrafish Vasa is required for germ-cell differentiation and maintenance. *Mol Reprod Dev* **81**, 946–61.
- Hay B, Jan LY and Jan YN (1990) Localization of Vasa, a component of *Drosophila* polar granules, in maternal effect mutants that alter embryonic anteroposterior polarity. *Development* **109**, 425–33.
- Hendriks S, Dancet EAF, van Pelt AMM, Hamer G and Repping S (2015) Artificial gametes: a systematic review of biological progress towards clinical application. *Hum Reprod Update* **21**, 285–96.
- Higaki S, Shimada M, Kawamoto K, Todo T, Kawasaki T, Tooyama I, Fujioka Y, Sakai N and Takada T (2017) *In vitro* differentiation of fertile sperm from cryopreserved spermatogonia of the endangered endemic cyprinid homnoroco (*Gnathopogon caeruleus*). *Sci Rep* **7**, 42852.
- Hodgson AN and Reunov AA (1994) Ultrastructure of the spermatozoon and spermatogenesis of the brachiopods *Disciniscia tenuis* (Inarticulata) and *Kraussina rubra* (Articulata). *Invert Reprod Dev* **25**, 23–31.
- Kalt MR (1973) Ultrastructural observations on the germ line of *Xenopus laevis*. *Z. Zellforsch* **138**, 41–62.
- Kashir J, Jones C, Child T, Williams SA and Coward K (2012). Viability assessment for artificial gametes: the need for biomarkers of functional competency. *Biol Reprod* **87**, 1–11.
- Kawasaki T, Saito K, Shinya M, Olsen LC and Sakai N (2010) Regeneration of spermatogenesis and production of functional sperm by grafting of testicular cell aggregates in zebrafish (*Danio rerio*). *Biol Reprod* **83**, 533–9.
- Kawasaki T, Saito K, Sakai C, Shinya M and Sakai N (2012) Production of zebrafish offspring from cultured spermatogonial stem cells. *Genes Cells* **17**, 316–25.
- Kawasaki T, Siegfried KR and Sakai N (2016) Differentiation of zebrafish spermatogonial stem cells to functional sperm in culture. *Development* **143**, 566–574.
- Kerr JB and Dixon KE (1974) An ultrastructural study of germ plasm in spermatogenesis of *Xenopus laevis*. *J Embryol Exp Morph* **32**, 573–92.
- Kloc M., Dougherty MT, Bilinski S, Chan AP, Brey E, King ML, Patrick CW Jr and Etkin LD (2002) Three-dimensional ultrastructural analysis of RNA distribution within germinal granules of *Xenopus*. *Dev Biol* **241**, 79–93.
- Knaut H, Pelegri F, Bohmann K, Schwarz H and Nüsslein-Volhard C (2000) Zebrafish *vasa* RNA but not its protein is a component of the germ plasm and segregates asymmetrically before germline specification. *J Cell Biol* **149**, 875–88.
- Kobayashi T, Kajiura-Kobayashi H and Nagahama Y (2000) Differential expression of Vasa homologue gene in the germ cells during oogenesis and spermatogenesis in a teleost fish, tilapia, *Oreochromis niloticus*. *Mech Dev* **99**, 139–42.
- Lacerda SM, Costa GM, and De França LR (2014) Biology and identity of fish spermatogonial stem cell. *Gen Comp Endocrinol* **207**, 56–65.
- Lasko PF and Ashburner M (1988) The product of the *Drosophila* gene *vasa* is very similar to eukaryotic initiation factor-4A. *Nature* **335**, 611–7.
- Leal MC, Cardoso ER, Nóbrega RH, Batlouni SR and Bogerd J (2009) Histological and stereological evaluation of zebrafish (*Danio rerio*) spermatogenesis with an emphasis on spermatogonial generations. *Biol Reprod* **81**, 177–87.
- Mahowald AP (1962) Fine structure of pole cells and polar granules in *Drosophila melanogaster*. *J Exp Zool* **151**, 201–5.
- Matova N and Cooley L (2001). Comparative aspects of animal oogenesis. *Dev Biol* **231**, 291–320.
- Mattei C and Mattei X (1978) La spermiogenese d'un poisson teleosteen (*Lepadogaster lepadogaster*). I. La spermatide. *Biol Cell* **32**, 257–66.
- Medrano JV, Reijo Pera RA and Simon C (2013). Germ cell differentiation from pluripotent cells. *Semin Reprod Med* **31**, 14–23.
- Meikar O, Ros MD, Korhonen H and Kotaja N (2011) Chromatoid body and small RNAs in male germ cells. *Reproduction* **142**, 195–209.
- Milani L, Pecci A, Ghiselli F, Passamonti M, Bettini S, Franceschini V and Maurizii MG (2017) VASA expression suggests shared germ line dynamics in bivalve molluscs. *Histochem Cell Biol* **148**, 157–71.
- Mochizuki K, Nishiyama-Fujisawa C and Fujisawa T (2001) Universal occurrence of the Vasa-related genes among metazoans and their germline expression in *Hydra*. *Dev Genes* **211**, 299–308.
- Moreno I, Miguez-Forjan JM and Simon C (2015) Artificial gametes from stem cells. *Clin Exp Reprod Med* **42**, 33–44.
- Muñoz M, Sàbat M, Mallol S, Casadevall M (2002) Gonadal structure and gametogenesis of *Trigla lyra* (Pisces: Triglididae). *Zool Stud* **41**, 412–20.
- Nikolic A, Volarevic V, Armstrong L, Lako M and Stojkovic M (2016) Primordial germ cells: current knowledge and perspectives. *Stem Cells Int* **2016**, 1741072.
- Onohara Y and Yokota S (2012) Expression of DDX25 in nuage components of mammalian spermatogenic cells: immunofluorescence and immunoelectron microscopic study. *Histochem Cell Biol* **137**, 37–51.
- Pek JW and Kai T (2011). A role for Vasa in regulating mitotic chromosome condensation in *Drosophila*. *Current Biology* **21**, 39–44.
- Raz E (2000) The function and regulation of Vasa-like genes in germ-cell development. *Genome Biol* **1**, 1–6.
- Reunov AA and Rice M (1993) Ultrastructural observations on spermatogenesis in *Phascolion cryptum* (Sipuncula). *Trans Am Microsc Soc* **112**, 195–207.
- Reunov AA and Klepal W (1997) Ultrastructural investigation of spermatogenesis in nemertine worm *Procephalothrix* sp. (Palaeonemertini, Anopla). *Helgoland Meer* **51**, 125–35.
- Reunov AA and Klepal W (2004) Ultrastructural study of spermatogenesis in *Phoronopsis harmeri* (Lophophorata, Phoronida). *Helgol Mar Res* **58**, 1–10.
- Reunov AA, Isaeva VV, Au DWT and Wu RSS (2000). Nuage constituents arising from mitochondria: is it possible? *Dev Growth Differ* **42**, 139–43.
- Reunov AA, Yurchenko OV, Alexandrova YN and Radashevsky VI (2010) Spermatogenesis in *Boccardiella hamata* (Polychaeta: Spionidae) from the Sea of Japan: sperm formation mechanisms as characteristics for future taxonomic revision. *Acta Zool* **91**, 447–56.
- Reunov AA, Alexandrova YN, Reunova YA, Komkova AV and Milani L (2018) Germ plasm provides clues on meiosis: the concerted action of germ plasm granules and mitochondria in the clam. *Zygote* **27**, 25–35.
- Riesco MF, Valcarce DG, Alfonso J, Herráez MP and Robles V (2014) *In vitro* generation of zebrafish PGC-like cells. *Biol Reprod* **91**, 1–11.
- Saffman EE and Lasko P (1999). Germline development in vertebrates and invertebrates. *Cell Mol Life Sci* **55**, 1141–63.
- Sakai N (2002) Transmeiotic differentiation of zebrafish germ cells into functional sperm in culture. *Development* **129**, 3359–65.
- Satoh N (1974) An ultrastructural study of sex differentiation in the teleost *Oryzias latipes*. *J Embryol Exp Morphol* **32**, 195–215.
- Schulz RW, de França LR, Lareyre J-J, LeGac F, Chiarini-Garcia H, Nóbrega RH and Miura T (2010) Spermatogenesis in fish. *Gen Comp Endocrinol* **165**, 390–411.
- Shang P, Baarends WM, Hoogerbrugge J, Ooms MP, van Cappellen WA, de Jong AAW, Dohle GR, van Eenennaam H, Gossen JA and Grootegoed JA (2010) Functional transformation of the chromatoid body in mouse spermatids requires testis-specific serine/threonine kinases. *J Cell Sci* **123**, 331–9.
- Strome S and Wood WB (1983) Generation of asymmetry and segregation of germ-line granules in early *C. elegans* embryos. *Cell* **35**, 11–25.
- Sunagara T, Saito Y and Kawamura K (2006) Postembryonic epigenesis of Vasa-positive germ cells from aggregated hemoblasts in the colonial ascidian *Botryllus primigenus*. *Dev Growth Differ* **48**, 87–100.
- Timmermans LPM and Taverne N (1989) Segregation of primordial germ cells: their numbers and fate during early development of *Barbus conchonioides* (Cyprinidae, Teleostei) as indicated by ³H-thymidine incorporation. *J. Morphol* **202**, 225–37.

- Toyooka Y, Tsunekawa N, Takahashi Y, Matsui Y, Satoh M and Noce T** (2000) Expression and intracellular localization of mouse Vasa-homologue protein during germ cell development. *Mech Dev* **93**, 139–49.
- Tzung K-W, Goto R, Saju JM, Sreenivasan R, Saito T, Arai K, Yamaha E, Hossain M., Calvert MEK and Orbán L** (2014) Early depletion of primordial germ cells in zebrafish promotes testis formation. *Stem Cell Rep* **4**, 61–73.
- Villegas J, Araya P, Bustos-Obregon E and Burzio LO** (2002) Localization of the 16S mitochondrial rRNA in the nucleus of mammalian spermatogenic cells. *Mol Hum Reprod* **8**, 977–83.
- Wilk K, Bilinski S, Dougherty MT and Kloc M** (2004) Delivery of germinal granules and localized RNAs via the messenger transport organizer pathway to the vegetal cortex of *Xenopus* oocytes occurs through directional expansion of the mitochondrial cloud. *Int J Dev Biol* **49**, 17–21.
- Williamson A and Lehmann R** (1996) Germ cell development in *Drosophila*. *Annu Rev Cell Dev Biol* **12**, 365–91.
- Wolf PM, Priess J and Hirsh D** (1983) Segregation of germline granules in early embryos of *Caenorhabditis elegans*. An electron microscopic analysis. *J Embryol Exp Morphol* **73**, 297–306.
- Xu H, Gui J and Hong Y** (2005) Differential expression of Vasa RNA and protein during spermatogenesis and oogenesis in the gibel carp (*Carassius auratus gibelio*), a bisexually and gynogenetically reproducing vertebrate. *Dev Dynam* **233**, 872–82.
- Yajima M and Wessel GM** (2011) The multiple hats of Vasa function and its regulation of cell cycle progression. *Mol Reprod Dev* **78**, 861–7.
- Yakovlev KV** (2016) Localization of germ plasm-related structures during sea urchin oogenesis. *Dev Dynam* **245**, 56–66.
- Yuan Y, Li M and Hong Y** (2014) Light and electron microscopic analyses of Vasa expression in adult germ cells of the fish medaka. *Gene* **545**, 15–22.